Thesis for the Degree of Master of Engineering

Combination of chemo-photothermal therapy against cancer using fucoidan-coated CuS nanoparticles

by

Bian Jang

Department of Interdisciplinary Program of Biomedical Mechanical & Electrical Engineering

The Graduate School

Pukyong National University

August 2017

Combination of chemo-photothermal therapy against cancer using fucoidan-coated CuS nanoparticles

(후코이단−황화구리 나노입자를 이용한 화학광열 암치료)

Advisor: Prof. Jung Hwan Oh

by

Bian Jang

A thesis submitted in partial fulfillment of the requirements
for the degree of Master of Engineering
in Interdisciplinary Program of Biomedical Mechanical & Electrical
Engineering,
The Graduate School,
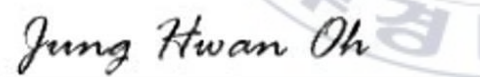**Pukyong National University**

August 2017

Combination of chemo-photothermal therapy against cancer

using fucoidan-coated CuS nanoparticles

A dissertation

by

Bian Jang

Approved by:

_____

SeungYun Nam

_____   _____

JungHwan Oh   MinSeok Kwak

August 25, 2017

LIST OF CONTENTS

Combination of chemo-photothermal therapy against cancer using fucoidan-coated CuS nanoparticles

Bian Jang

Interdisciplinary Program of Biomedical Mechanical & Electrical Engineering,

The Graduate School,

Pukyong National University

Abstract

In advanced cancer therapy, the combinational therapeutic effect of photothermal therapy (PTT) using near-infrared (NIR) light-responsive nanoparticles (NPs) and anti-cancer drug delivery-mediated chemotherapy has been widely applied. However, chemo–phototherapy has no beneficial effect in the systemic prevention of cancer, since anti-cancer drugs promote cancer cell necrosis. In this study, through a facile, low-cost, and solution-based method, we develop and synthesize fucoidan, a natural polymer isolated from seaweed that shows anti-cancer effect, and coated it on NPs as an ideal candidate in chemo–photothermal therapy against cancer cells. Fucoidan-coated copper sulfide nanoparticles (F-CuS) act not only as a nanocarrier to enhance the intracellular delivery of fucoidan, but also as a

photothermal agent to effectively ablate different cancer cells (e.g., HeLa, A549, and K562), both *in vitro* and *in vivo*, with the induction of apoptosis under 808 nm diode laser irradiation. These results guarantee the potential usage of F-CuS in treating human cancer.

Keywords: Fucodian, CuS NPs, Photothermal Therapy, Apoptosis, Necrosis, Chemotherapy
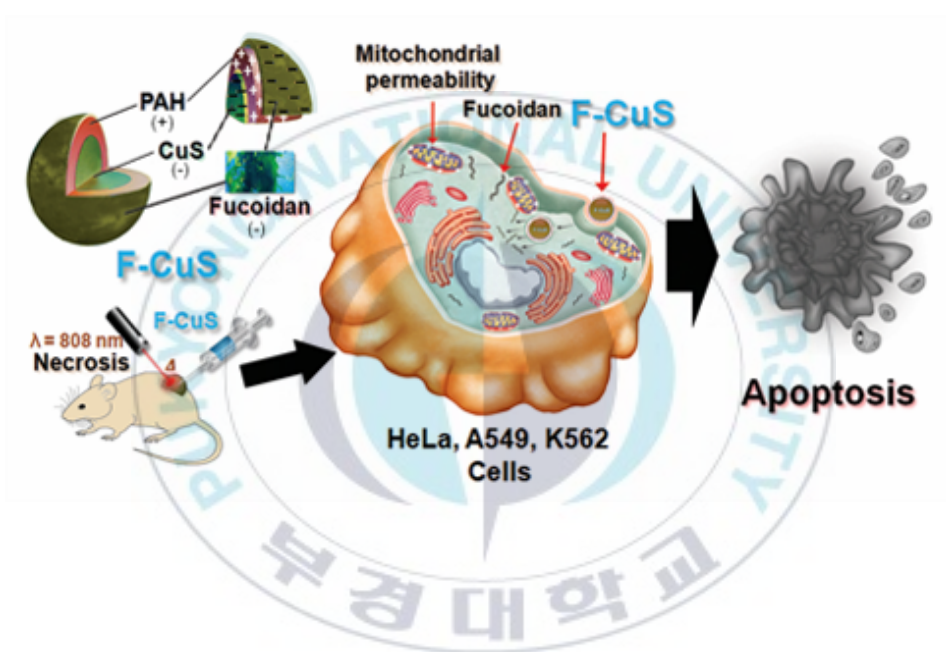
후코이단-황화구리 나노입자를

이용한 화학광열 암치료

장 비 안
부 경 대 학 교   대 학 원
의생명기계전기융학공학협동과정

초   록

효과적인 암 치료를 위하여 근적외선 파장 대에 반응하는 나노입자를 이용한 광열치료와 항암제를 사용한 약물요법을 함께 적용하는 병용요법이 최근 활발히 사용되고 있다. 하지만 지금까지의 이러한 병용요법은 암세포의 세포자멸사가 아닌 세포괴사를 유도하여 암세포를 제거하는 것에 초점을 두었기에 암세포의 전이나 재발을 막지 못할 뿐만 아니라 세포괴사를 유도하여 다른 건강한 세포 및 조직의 염증을 유도하는 등 여러 한계점을 보여주었다. 이번 논문 실험에서는 808nm 파장대 빛을 흡수하여 열을 내는 황화구리 나노입자에 후코이단이란

탁월한 항암효과를 가진 해양 천연 고분자를 화학적 약물 대신 코팅하여 세포괴사가 아닌 암세포자멸사를 유도하는 물질을 합성하였다. 후코이단-황화구리 나노입자의 광열치료효과와 약물치료효과를 자궁경부암 세포 HeLa, 폐암세포 A549, 그리고 백혈병 세포 K562 를 대상으로 실험했고, 후코이단-황화구리 나노입자의 탁월한 암치료효과를 증명할 수 있었다. 세포실험을 바탕으로 세 종류의 암세포를 누드마우스에 이식하여 치료하는 동물실험을 추가로 진행하여 후코이단-황화구리 나노입자의 치료효과를 보다 깊이 연구하고 증명하였다.

List of Figures and Table

Chapter 1. Introduction

1.1. Fucoidan: structure and biological activity

For the successful cancer treatment, many anti-cancer drugs have been developed, investigated and applied in practice. Despite the efforts, chemotherapy have faced some limitations, such as unaffected side-effects [1]. Since some natural products show efficient anti-cancer effect without any toxicity in normal cells or side effect, it holds the limelight as an alternative for chemical drugs [2]. Fucoidan, a sulfated polysaccharide extracted from marine brown seaweed and some marine invertebrates, such as sea urchins and sea cucumbers, was first isolated from brown seaweed by Kylin in 1913 [3]. Even though the chemical structure of fucoidan vary depend on the species of marine seaweed that used to prepare fucoidan, it is mainly composed of fucose and sulfate [4]. Fucoidan extracted from *Fucus Vesiculosus,* the most common and widely used commercial product, is composed of 44.1% of fucose, 26.3% of sulfate and 31.1% of ash with small amount of aminoglucose [5]. The chemical structure of Fucoidan of *F. Vesiculosus* suggested by Pankter *et al* in 1993 has α-(1→3) linked fucose in the core chain and substituted sulfate at C-4 of main chain with fucose attached to some fucose residues along the main chain (Figure 1) [6].

1
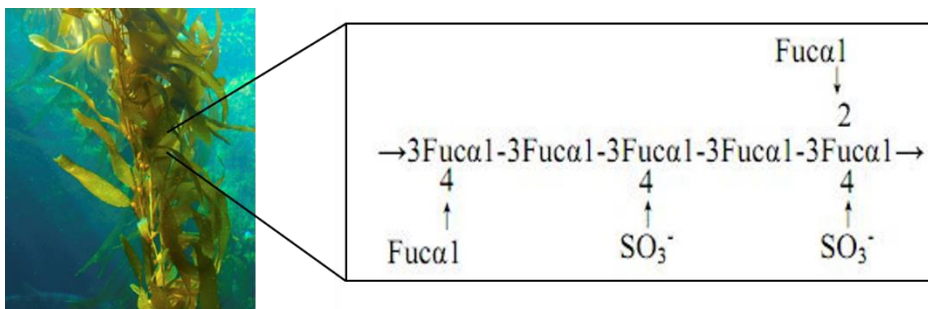
Figure 1. The chemical structure of fucoidan of *F. Vesiculosus* by Kankter. Adapted from "A revised structure for fucoidan may explain some of its biological activities" by M.S. Patankar, S. Oehninger, T. Barnett, R.L. Williams, G.F. Clark, 1993, Journal of Biological Chemistry, 268(29), 21770-21776. Copyright 1993 Journal of Biological Chemistry.

Due to the diversity of fucoidan sources and seaweed species, researchers face difficulty of the complete structural analysis for all kinds of fucoidan. However, there are some fucoidan that have been revealed for its chemical composition (Table 1) [7].

Brown seaweed species	Chemical composition
F. vesuculosus	fucose, sulfate
F. evanescens C.Ag.	fucose/sulfate/acetate (1/1.23/0.36)
F. distichus	fucose/sulfate/acetate (1/1.21/0.08)
F. serratus L.	fucose/sulfate/acetate (1/1/0.1)
Lessonia vadosa	fucose/sulfate (1/1.12)
Macrocytis pyrifera	Fucose/galactose (18/1), sulfate
Pelvetia weightii	Fucose/galactose (10/1), sulfate

Undaria pinnatifida	Fucose/galactose (1/1.1), sulfate
Ascophyllum nodosum	Fucose(49%), GlcA(11%), Xylose(10%), sulfate
Laminaria angustata	Fucose/galactose/sulfate (9/1/9)
Himanthalia lorea and Bifurcaria bifurcate	Fucose, GlcA, Xylose, sulfate
Adebicytis utricularis	Fucose, mannose, galactose, sulfate
Padina pavonia	Fucose, mannose, xylose, glucose, galactose, sulfate
Ecklonia kurome	Fucose, mannose, xylose, galactose, GlcA, sulfate
Sargassum stenophyllum	Fucose, mannose, xylose, galactose, GlcA, glucose, sulfate
Hizikia fusiforme	Fucose, mannose, xylose, galactose, GlcA, sulfate
Dictyota menstrualis	Fucose/xylose/uronic acid/ galactose/sulfate (1/0.8/0.7/0.8/0.4)
Spatoglossum schroederi	Fucose/xylose/galactose/sulfate (1/0.5/2/2)

Table 1. Chemical composition of fucoidan from different sources. Adapted from "Fucoidan: structure and bioactivity" by B. Li, F. Lu, X. Wei, R. Zhao, 2008, Molecules, 13(8), 1671-95.

Among other natural polymers from marine, fucoidan is well-known for various biological effects and numerous biological activities such as anti-coagulant, anti-virus, and anti-cancer and immune modulation [8-12]. Especially, anti-cancer effect of fucoidan against various types of cancer,

including breast cancer, lung cancer, cervical cancer, and leukemia, has already been well defined [11, 13-15]. In addition, due to the possession of functional groups (-OH, or -SO$_3$), fucoidan is widely used to conjugate with or modify the surface of nanoparticles [16]. Therefore, research about fucoidan conjugated nanoparticles for drug delivery in anti-cancer therapy is actively ongoing [17, 18].

1.2. Photothermal Therapy

Photothermal therapy (PTT), an emerging alternative or supplement of conventional cancer treatments, has outstanding advantages, such as minimal invasion, cancer site specificities and fast recovery [19]. PTT employs a near-infrared light (NIR) source and a photoabsorber which absorbs and converts light energy into heat to ablate the cancer cells. As the interest for PTT grows, various NIR responsive inorganic NPs have been developed, such as gold NPs, carbon nanotubes, and copper sulfide nanoparticles (CuS), and some NPs which have proven its therapeutic effect and biocompatibility are under clinical trials [20-22]. In PTT, NPs are delivered to cancer cells by intratumoral or intravenous injection. When the light are exposed at tumor site, injected nanoparticles produce heat by synchronized oscillation of electrons and they increase the temperature of tumor for the ablation of cancer [20]. Here, the temperature increase depends on various factors, such as the photothermal conversion efficiency

of NPs, the concentration of NPs delivered into tumor, and the power of laser power which used as NIR light. When synthesizing the NPs, not only photothermal conversion efficiency and biocompatibility but also photostability and cost-effectiveness need to be considered. Among many criteria, the possession of absorbance in NIR wavelength of light (700-1100nm), since it can penetrate deeply than visible light wavelength through biological tissues and do not absorbed by water of blood, is one of the most important one for NPs to act as a photoabsorber [23]. CuS, which show great biocompatibility, photothermal conversion efficiency, photostability within the size of 3–30 nm and low cost for synthesis, satisfy the requirements as a photothermal agent [24].

1.3. PTT-induced Apoptosis

Induction of apoptosis, also called programmed cell death, which plays a key role in the successful cancer treatment. This is because apoptotic bodies, which are produced through the mitochondria dependent/independent apoptosis signaling pathways, can be phagocytosed by dendritic cells and macrophages and consequently promote cancer antigen-specific immune activation and prevent tumor growth [25, 26]. In contrast to apoptosis, necrosis process is unable to induce immune activation and may cause some serious side effects including inflammation (Figure 2) [25, 27].

5
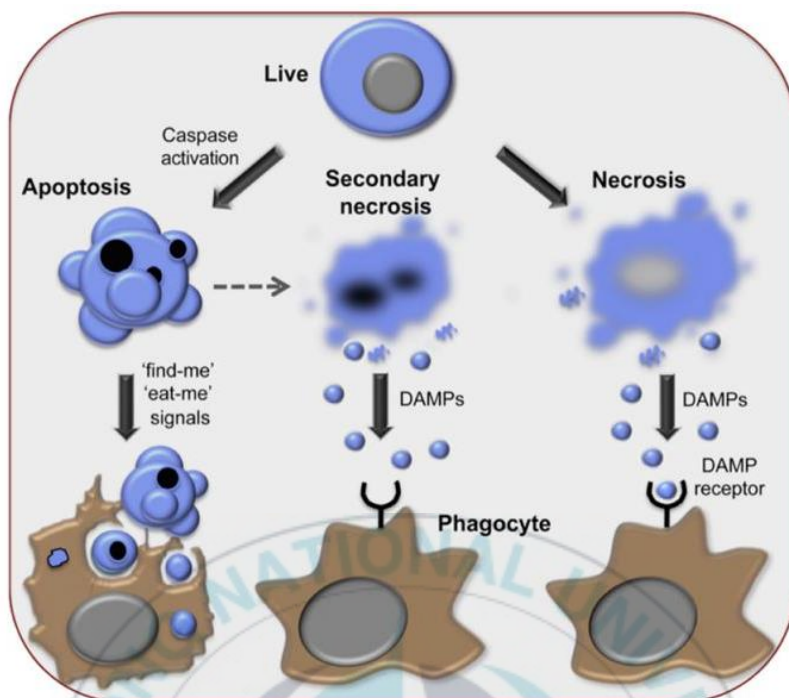
Figure 2. The two mechanisms of cell death: apoptosis and necrosis. Cells undergone apoptosis preserve their membranes and forms apoptotic bodies which can be phagocytosed by dendritic cells for immune response without inflammation. Apoptosis may lead to secondary necrosis which cause loss of cell membrane and release damage-associated molecular patterns (DAMPs) without phagocytosis. Contrast to apoptosis, necrosis cause the destruction of membrane and release DAMPs which cause inflammation. Adapted from "Elucidating the fundamental mechanisms of cell death triggered by photothermal therapy" by J.R. Melamed, R.S. Edelstein, E.S. Day, 2015, ACS Nano, 9(1), 6-11. Copyright 2012 Elsevier.

Recently, to improve the therapeutic effect against cancer, a combination of chemotherapy and PTT, chemo-photothermal therapy has

6

widely studied and gained great interests due to the synergetic treating effect and the noticeable improvement of drug uptake as NPs can easily enter into cells through phagocytosis [28-30]. However, previous studies about this combinational therapy have only focused on the induction of cancer cell death, but have not evaluated whether cell death were caused by apoptosis or necrosis. Therefore, induction of apoptosis by the combination of chemotherapy and PTT against cancer cells needs to be carefully investigated to minimize the side effects of necrosis and this may be one of the most effective therapeutic methods to treat the cancer.

In this study, we introduce a facile electrostatic method to synthesize small and highly biocompatible fucoidan-coated copper sulfide nanoparticles (F-CuS) that could serve as a novel candidate in chemo–photothermal therapy. We hypothesized that since F-CuS may promote cancer-cell apoptosis through the improved intracellular delivery of fucoidan and the photothermal effect of NIR irradiation, our system will effectively eliminate cancer cells and prevent tumor growth. Experiments were undertaken to prove the hypothesis against HeLa, a human cervical cancer cell line, and A549, a human lung cancer cell line, both *in vitro* and *in vivo*. In addition, we also evaluated the therapeutic effect of F-CuS against K562, a leukemia cell line, which is resistant against a number of drugs, including fucoidan [11, 31].

Chapter 2. Materials and Methods

2.1. Materials and measurement

All chemicals were purchased form Sigma Aldrich Chemical, Inc. (St. Louis, MO, USA), unless otherwise specified. Sodium Citrate ($C_6H_5O_7Na_3 \cdot 2H_2O$) was purchased from the DC Chemical Co. Ltd (Seoul, South Korea). Field emission transmission electron microscopy (FE-TEM) and electron diffraction (ED) pattern images were taken with a JEM-2100F transmission electron microscope (JEOL; Tokyo, Japan). FT-IR spectra were measured with a Spectrum GX (PerkinElmer Inc.; Waltham, MA, USA). Power X-ray diffraction grapes were measured by an X'Pert-MPD System (Philips; Amsterdam, Netherlands). Dynamic light scattering and zeta potential measurements were taken with an ELS-8000 (Otsuka Electronics Co. Ltd.; Osaka, Japan). A thermogravimetric analyzer (TGA 7, Pyris 1; PerkinElmer Inc.; Waltham, MA, USA) was used to analyze the fucoidan coating and its concentration. UV-vis absorption spectra were recorded UV-Visible spectrophotometer (Beckman Coulter; Fullerton, CA, USA). A fiber-coupled continuous-wave diode laser (808 nm, 10 W) was purchased from Changchun New Industries Optoelectronics Technology Co., Ltd. (Changchun, China). Thermographic images were taken using a FLIR ONE (FLIR Systems, Wilsonville, OR, USA). Intracellular

fluorescence imaging was observed by using a Leica laser scanning confocal microscope (Leica Microsystems; Wetzlar, Germany). Flow cytometry analysis data were obtained by using a BD LSR Fortessa (Becton Dickinson; Coppelle, TX, USA).

2.2. Preparation of F-CuS

Citrate-stabilized copper sulfide nanoparticles were synthesized according to a previously published report [32]. To coat PAH onto CuS [33], to a beaker containing 50 mL of PAH solution (Mw=17500, 2 mg/mL) we added, in a dropwise manner, crude CuS solution (50 mL) under sonication; the mixture was stirred for 4 h. To isolate PAH-CuS, the mixture was centrifuged at 19,000 rpm for 5 h; the dark green pellet was resuspended in 50 mL DI water. The fucoidan coating onto PAH-CuS was performed according to the literature, with slight modification [34]. PAH-CuS (50 mL) was added, in a dropwise manner, to 50 mL of fucoidan solution (1 mg/mL) under vigorous stirring. Again, centrifugation was performed to isolate the F-CuS pellet, which was resuspended in a stock solution (5 mg/mL). F-CuS used throughout all experiments herein were from single batch.

2.3. Mice

Six-week-old BALB/c nu/nu (nude) mice were obtained from the Shanghai Public Health Clinical Center and kept under pathogen-free conditions. The mice were maintained at a controlled temperature of 20–22 ℃, humidity of 50–60%, and 12:12-h lighting, with free access to standard rodent chow and water. All experiments were carried out in agreement with the guidelines of the Institutional Animal Care and Use Committee at the Shanghai Public Health Clinical Center. The protocol was approved by the Committee on the Ethics of Animal Experiments for the Shanghai Public Health Clinical Center (Mouse Protocol Number: SYXK-2010-0098). Mice were sacrificed through CO_2 inhalation euthanasia, and all efforts were made to minimize suffering.

2.4. Cells

HeLa, A549, and K562 cells were provided by the American Type Culture Collection (Rockwile, MD, USA). The cells were cultured in RPMI 1640 medium (Gibco; Paisley, UK) that was supplemented with 10% fetal calf serum (Gibco; Paisley, UK), 120 mg/L penicillin, and 200 mg/L streptomycin at 37 ℃ and 5% CO_2.

2.5. *In vitro* photothermal treatment

HeLa and A549 cells (1×10^5) were seeded into a 24-well plate for 24 h; they were then treated with fucoidan, CuS, or F-CuS for 2 h, and the cells were irradiated for 5 min with an 808 nm laser at 2 W/cm^2. In the case of the K562 cells, the cells were irradiated for 5 min at 2.5 W/cm^2.

2.6. MTT (3-(4,5-Dimethylthiazol-2-yl)-2,5-Diphenyltetrazolium Bromide) assay

The cultured cells were added with 100 μL of freshly prepared MTT solution (5 mg/mL in phosphate buffered saline [PBS]) and incubated for 4 h at the cell incubator. After incubation, the cells were lysed by 100 μL of DMSO at shaking incubator for 4 h. Absorbance was read at 620-nm, using an ELISA reader (Labsystems Multiskan; Roden, Netherlands).

2.7. Annexin-V and 7AAD staining

Cultured cells were stained with annexin V-FITC and 7AAD in 100 μL of binding buffer for 15 min at room temperature (RT). After 400 μL of binding buffer was added, the cells were analyzed by flow cytometry using a FACS Aria II (Becton Dickinson; San Diego, CA, USA).

2.8. Mitochondrial permeability assay

HeLa and K562 cells (2×10^6/ml) were treated with 40 nM of 3,3'-dihexyloxacarbocyanine iodide (DiOC$_6$(3); Sigma-Aldrich, St. Louis, MO, USA) for 30 min at 37 ℃ and then washed with PBS. Stained cells were analyzed by flow cytometry.

2.9. Analysis of Caspase 3 activation

The activation of caspase-3 was determined with a CaspGLOWTM Red Active Caspase-3 Staining Kit (BioVision; Milpitas, CA, USA), according to the manufacturer's protocols. Briefly, the cells were incubated with active caspase-3 staining reagent for 30 min at RT. After washing with washing buffer, the cells were resuspended with 500 μL PBS and analyzed by flow cytometry.

2.10. *In vivo* photothermal treatment

Nude mice were *s.c.* injected with 5×10^6 HeLa, A549, or K562 cells. Once tumors at their longest dimension reached a size of ~5.0 mm, mice were randomized into six treatment groups: PBS, fucoidan, F-CuS, PBS with laser treatment, CuS NPs with laser treatment, and F-CuS with laser treatment. Each NP type was *i.t.* injected into the mice. Two hours after injection, an 808 nm NIR laser was applied to irradiate tumors under a

power intensity of 2 W/cm^2 (Hela and A549) or 2.5 W/cm^2 (K562). The temperature was recorded using an infrared camera FLR One Thermal imaging system (FLIR; Wilsonwille, OR, USA). Tumor volume was calculated by using the formula V ¼ 1/2 (L/S2), where L is the longest dimension and S is the shortest dimension.

2.11.   Statistical analysis

All statistical analysis results are expressed as the mean ± standard error of the mean. The statistical significance of differences between experimental groups was calculated using analysis of variance, and either a Bonferroni posttest or an unpaired Student's t-test. All p-values < 0.05 were considered significant.

3. Results and discussion

3.1. Preparation and Characterization of F-CuS NPs

We first synthesized sodium citrate-stabilized copper sulfide nanoparticles (CuS) and coated the NPs by using the layer-by-layer (LbL) technique, by alternating poly-cationic and anionic substances (i.e., poly (allylamine hydrochloride) (PAH) and fucoidan (Figure 3)) [32, 33].
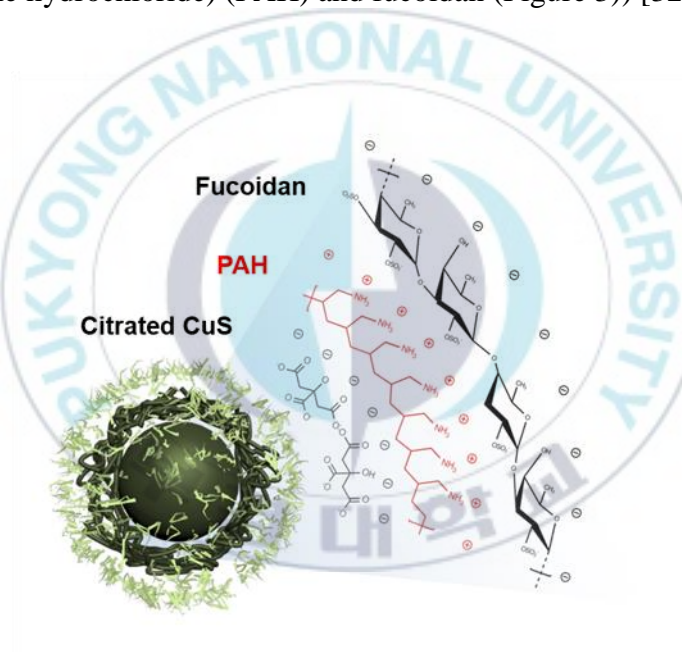
Figure 3. Graphical structure of F-CuS prepared for chemo- and photothermal cancer therapy.

The intermediate adhesive layer, the PAH coating, not only improves the stability of NPs [34], but also acts as a linker by introducing the positively

charged functional group onto the negatively charged CuS surface [33].

Then, fucoidan was coated onto the surface of PAH-CuS by creating a

strong electrostatic interaction between PAH (NH_3^+) and fucoidan (SO_3^-).

Additionally, we hypothesized that the LbL-fabricated NPs could be pH-

responsive within cancerous cells [18, 35]. On transmission electron

microscopy images, we observed spherical CuS and F-CuS with an average

size of 10 nm (Figure 4a and b). X-ray diffraction and ED pattern were used

to determine and confirm the crystallization and purity of synthesized CuS,

relative to standard data from the Joint Committee on Powder Diffraction

Standards card (06-0464). The strong and sharp peaks prove the fair

crystallinity of the synthesized NP, while the lack of other peaks indicates

that the substance is highly pure (Figure 4c).
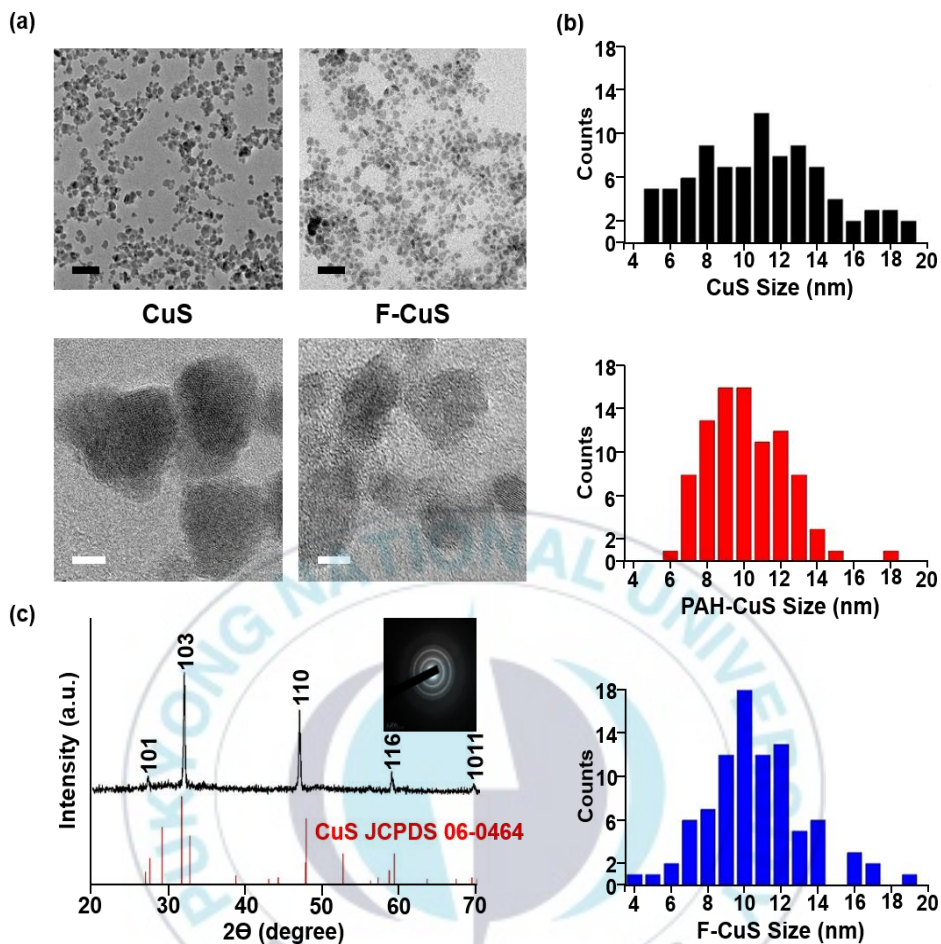
Figure 4. Morphological characteristics of F-CuS. (a) FE-TEM images of CuS and F-CuS. Scale bars: 50 nm (black) and 5 nm (white). (b) TEM corresponding size distribution histogram of each coated nanoparticles: CuS (black), PAH-CuS (red), F-CuS (blue). (c) XRD and ED pattern (inset) of CuS with the standard JCPDS card 06-0464 of CuS.

Successful coatings of PAH and fucoidan onto CuS were confirmed by performing Fourier-transform infrared spectroscopy (FT-IR) and examining zeta potential. As shown in Figure 5a, all three FT-IR spectra showed the Cu-S stretching at 614 cm^{-1}. Since the citrate worked as a stabilizer in CuS, peaks indicating C–O (1114 cm^{-1}), O–H (1389 cm^{-1}), and C=O (1626 cm^{-1}) were present in the CuS spectra. After applying the PAH coating onto the CuS, a new peak appeared at 1498 cm^{-1}, indicating the bending mode of amine (N–H). After applying the fucoidan coating onto PAH-CuS, the formation of new peaks of S=O (840, 1230 cm^{-1}) and a saccharide ring (1024 cm^{-1}) were detected, which indicate the presence of fucoidan. In addition, zeta potential values changed from –39.12 mV (CuS) to +46.47 mV (PAH-CuS) and –35.91 mV (F-CuS), after each coating of PAH and fucoidan, respectively (Figure 5b). Thus, these data indicate that CuS had been successfully coated with PAH and fucoidan.

17
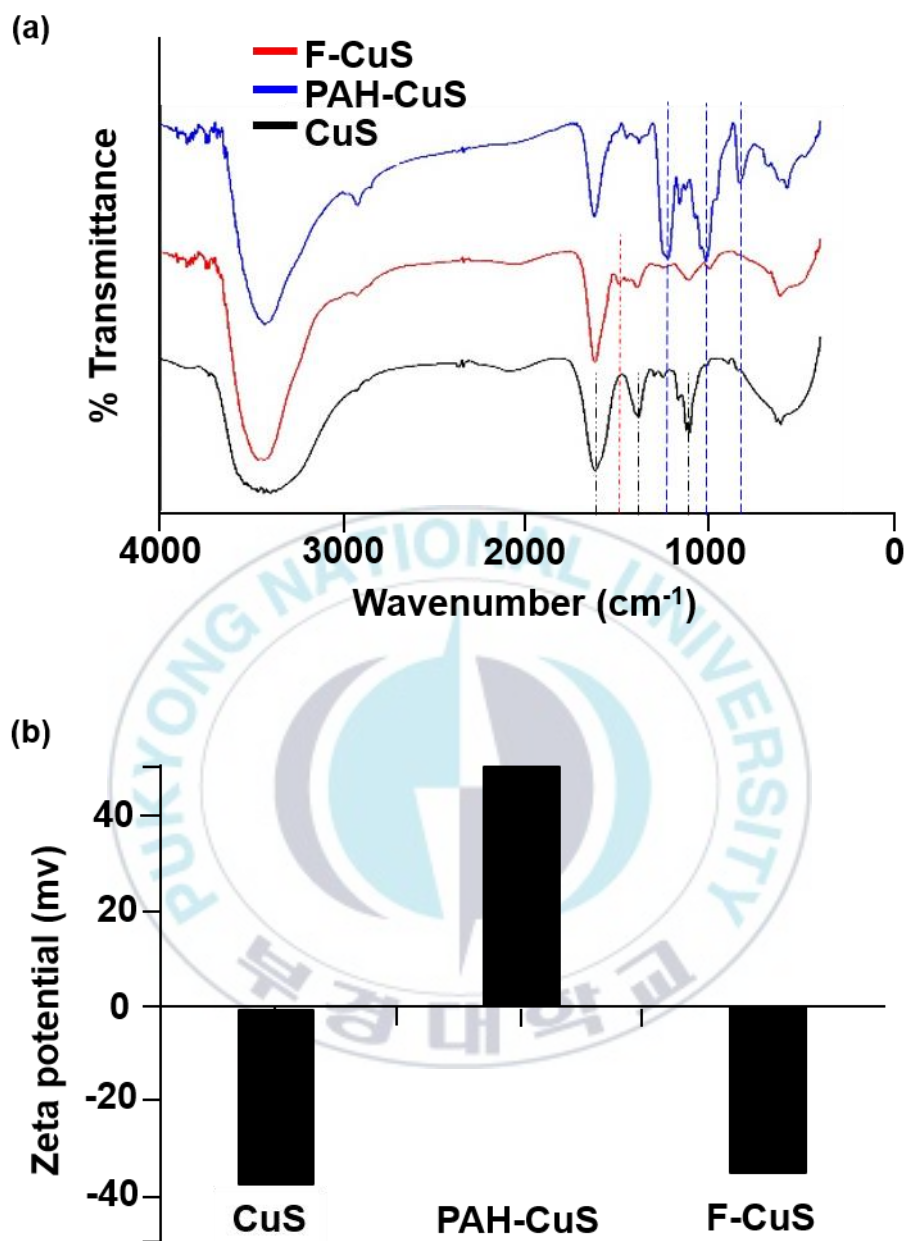
Figure 5. Coating of Fucoidan onto CuS. (a) FT-IR spectra of CuS (black),

PAH-CuS (red), and F-CuS (blue). (b) Zeta potential value of each NP.

3.2. Photothermal property of F-CuS

One of the most remarkable features of CuS is the broad and strong absorption in the NIR region (700–1100 nm) to utilize heat generated by the vibrational energy of the d–d transition of Cu^{2+} (Figure 6a). To evaluate the photothermal effect, the temperature of aqueous F-CuS samples at different concentrations were measured under laser irradiation (2 W/cm^2) at 808 nm for 5 min. As anticipated, higher concentrations lead to higher temperature increases under NIR irradiation, where 50 and 100 μg/mL F-CuS solutions reached 50 ℃ within 4 and 3 min, respectively; the PBS-mediated temperature increase, in comparison, was only 5 ℃ in 5 min (Figure 6c). In addition, to confirm the photostability of F-CuS, its absorption spectra were measured before and after the laser irradiation, and no marked difference in the spectra was observed (Figure 6b). Therefore, we concluded that the F-CuS system is a good candidate for PTT material, given its proven stability under experimental conditions.
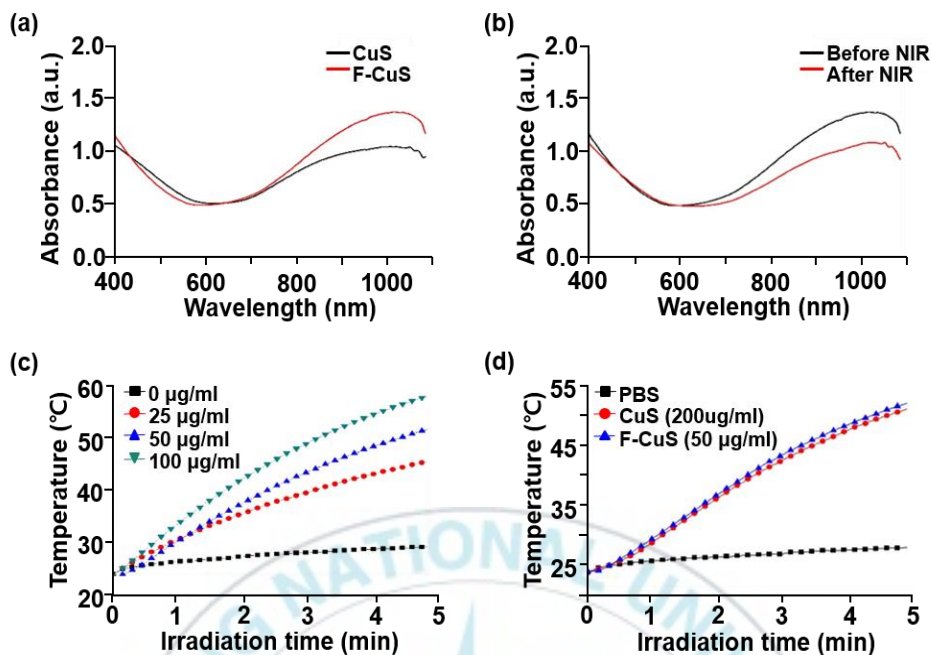
Figure 6. Photothermal properties of F-CuS. (a) UV-vis absorption of CuS (black) and F-CuS (red). (b) UV-vis absorption of F-CuS before (black) and after (red) NIR-irradiation. (c) Photothermal heating curves of different concentrations of F-CuS dissolved in water, irradiated for 5 min with an 808 nm laser at a power density of 2 W/cm^2. (d) photothermal heating curves of CuS (red) and F-CuS (blue) with different concentration dossolved in PBS irradiated using 808 nm laser with power density of 2W/cm^2 for 5 min.

3.3. F-CuS mediated anti-cancer effect *in vitro*

Since NPs generally exhibit improved drug delivery *in vitro* and *in vivo*, one can speculate that fucoidan can be effectively delivered to the intracellular environment. To quantify the amount of coated fucoidan, thermogravimetric analysis (TGA) was performed; we found that the estimated mass of fucoidan compared to the total mass of F-CuS was ~10 wt% (Figure 7).
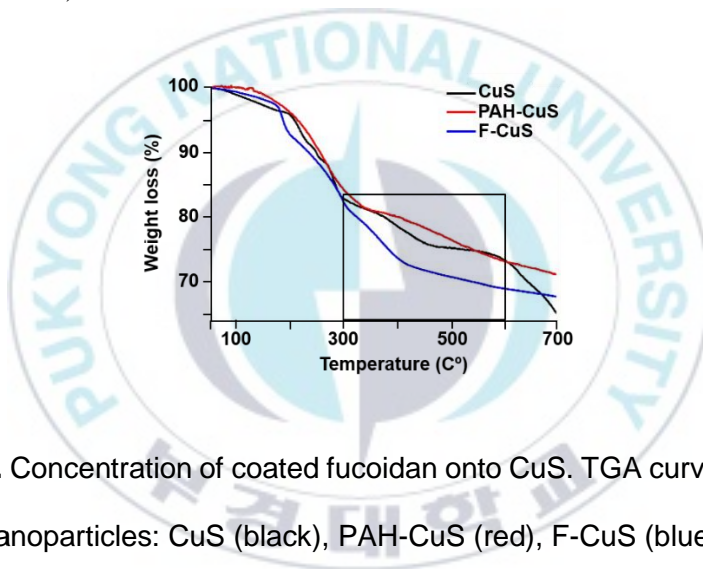
Figure 7. Concentration of coated fucoidan onto CuS. TGA curves of each coated nanoparticles: CuS (black), PAH-CuS (red), F-CuS (blue).

Next, we also examined whether F-CuS is more efficient in delivering fucoidan to cancerous cells than fucoidan alone. We prepared fluorescein isothiocyanate (FITC)-labelled fucoidan and F-CuS, separately, to detect by fluorescence microscopy the intracellular uptake of the two materials. HeLa cells were treated with 75 ng/mL fucoidan-FITC or 50 µg/mL F-CuS-

FITC. Here, the concentration of fucoidan was set to the estimated amount of fucoidan coated onto the working concentration of F-CuS (*i.e.*, 50 µg/mL). Two hours posttreatment, we characterized the intracellular uptake of fucoidan and observed that FITC fluorescence signals as per confocal laser scanning microscopy (Figure 8a) and flow cytometry (Figure 8b) were substantially higher in F-CuS-FITC-treated HeLa cells than those treated with fucoidan-FITC (Figures 8a and b). These data suggest that NP formulation may play an important role in the intracellular uptake of fucoidan into cancerous cells.
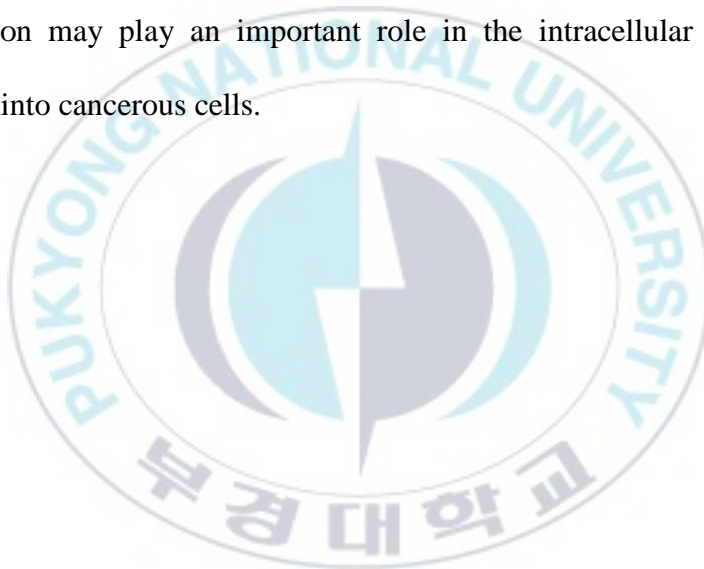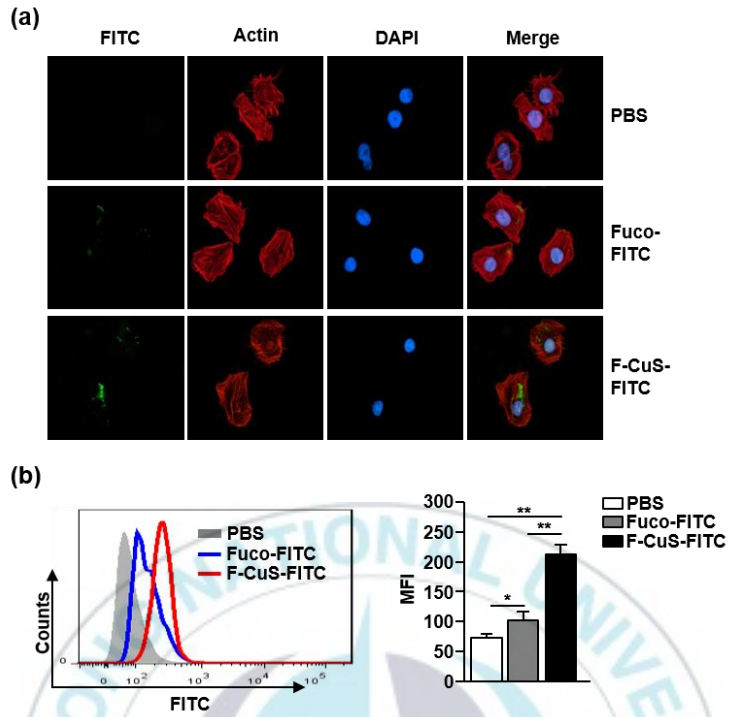
Figure 8. Intracellular uptake of fucoidan in HeLa cells by F-CuS. (a) HeLa cells (2×10^5) were incubated with fucoidan-FITC and F-CuS-FITC for 2 h. The cells were then stained with β-actin and 4',6-Diamidino-2-Phenylindole, Dihydrochloride (DAPI). The FITC expression levels were measured with a confocal microscope. (b) HeLa cells (2×10^5) were incubated with fucoidan-FITC (Fuco-FITC) and F-CuS-FITC for 2 h. The intracellular uptake of fucoidan was analyzed on a flow cytometry (left panel). Mean fluorescence intensity (MFI) of FITC positive cells was shown (right panel), * $p < 0.05$, ** $p < 0.01$. Data are representative of or the average of analyses of 6 independent samples (2 samples per experiment, 3 independent experiments).

23

To this end, we examined the anti-cancer effect of F-CuS. First, HeLa cells were incubated with an indicated concentration of F-CuS for 2 h, and subsequently irradiated for 5 min, using an 808 nm laser with a power intensity of 2 W/cm^2. Cell viability moderately decreased (60–80%) following treatments with 50 and 100 μg/mL F-CuS without NIR irradiation (Figure 9a). Interestingly, NIR irradiation of F-CuS-treated HeLa cells reduced their viability to 60%, even in the case of the 25 μg/mL F-CuS treatment. Furthermore, NIR treatments with higher concentrations of F-CuS (i.e., 50 and 100 μg/mL) showed almost complete killing of the cells (Figure 9a).
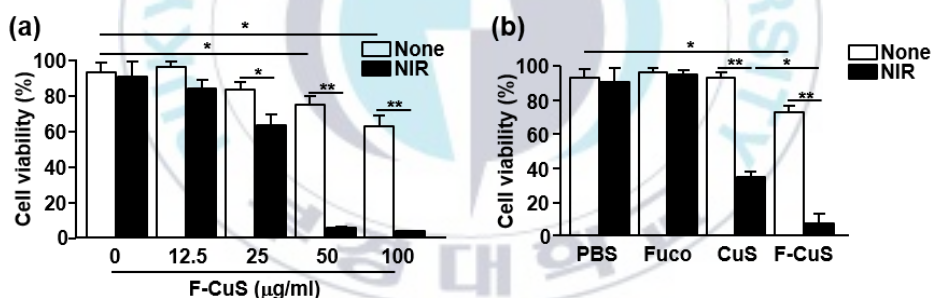
Figure 9. *In vitro* chemo–photothermal therapy by F-CuS. (a) HeLa cells were treated with an indicated concentration of F-CuS, and the cells were irradiated for 5 min with an 808 nm laser. Cell viability was analyzed by MTT assay. (b) MTT analysis of fucoidan, CuS, and F-CuS-treated HeLa cells with or without NIR irradiation.

Next, we evaluated whether fucoidan coating on CuS is beneficial in killing HeLa compared to CuS without the coating. Since LbL coatings onto CuS with additional materials, such as PAH and fucoidan, change the total mass of substances in solution, we fixed the hyperthermia parameter by adjusting the concentration of CuS (200 μg/mL) and F-CuS (50 μg/mL) to reach the same temperature (50 ℃), under identical irradiation conditions (Figure 6d). Here, it should be noted that the concentration of CuS was higher than that of F-CuS; this is because CuS cannot be isolated by centrifugation, whereas F-CuS can be; thus, the freeze-dried weight containing residual chemicals was used to back-calculate the concentration of crude CuS. In addition, the concentration of fucoidan alone (Fuco) was set to 75 ng/mL—the estimated amount of fucoidan coated onto the working concentration of F-CuS. HeLa cells incubated with Fuco, CuS, or F-CuS for 2 h were again treated with NIR under identical conditions, and the resulting cell viability was determined. First, it was immediately apparent that the presence of CuS upon NIR irradiation resulted in significant cell death (Figure 9b), due to hyperthermia. Interestingly, under NIR irradiation, F-CuS-treated cells exhibited three times lower cell viability than CuS-treated ones; this can be interpreted as indicative of the synergistic effect of the chemo-agent and elevated temperature. Additionally, consistent with the data regarding the intracellular uptake of

25

fucoidan alone and F-CuS (Figure 8), fucoidan alone was found to have failed in inducing cell death, as fucoidan alone cannot be effectively delivered into the cells.

3.4. Synergistic anti-cancer effects of F-CuS by hyperthermia upon NIR irradiation, and enhanced apoptosis caused by fucoidan

To derive successful tumor elimination, the induction of apoptosis is essential, since apoptotic cells promote the activation of tumor antigen-specific immune responses, including cytotoxic T lymphocyte activation [25, 26]. Apoptosis is characterized by DNA fragmentation, mitochondrial damage, and phosphatidylserine exposure in the cells [36]. Fucoidan has already been found to induce apoptosis in both HeLa and A549 cells, which appear in different human organs (*i.e.*, the cervix and lung, respectively) [13, 37, 38]. Therefore, we examined annexin-V and 7AAD staining to determine apoptosis and necrosis, respectively. The agreed-upon MTT assay for HeLa—namely, 50 and 100 µg/mL F-CuS treatments without NIR irradiation—induced slight increases in early apoptosis and late apoptosis/necrosis (Figure 10a); NIR irradiation promoted dramatic increases in apoptotic cells in the 50 µg/mL F-CuS treatment (Figure 10a). Importantly, under NIR irradiation, 100 µg/mL F-CuS induced great increases in late apoptosis/necrosis, but showed an obviously low effect in

the promotion of early apoptosis compared to the 50 µg/mL F-CuS treatment (Figure 10a). NIR irradiation in the CuS-treated cells also induced a significant elevation of late apoptosis/necrosis compared to non-irradiated controls, but the early-apoptotic cell percentages were markedly lower than those of the F-CuS-treated ones (Figure 10b).
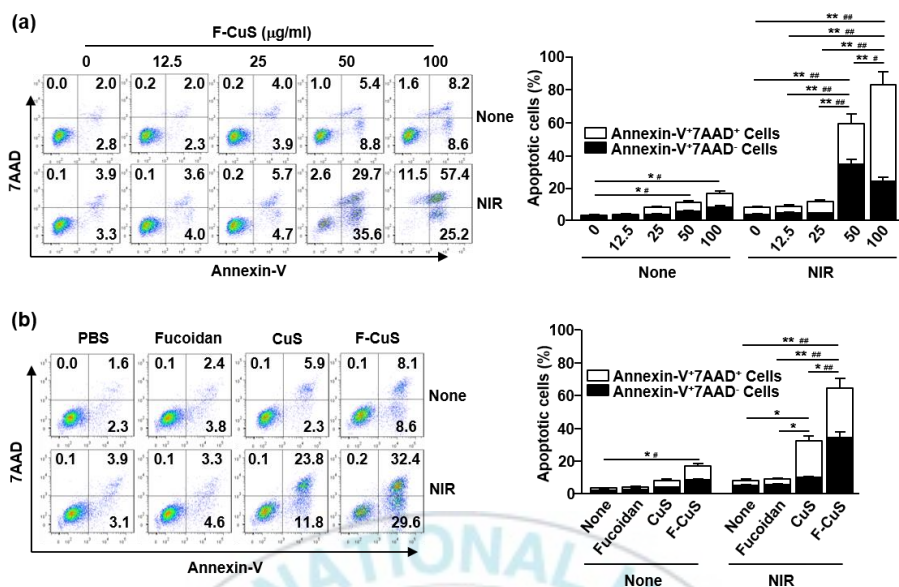
Figure 10. Apoptotic effect of F-CuS with laser irradiation against HeLa cells. (a) Dose-dependent apoptotic effect of F-CuS with or without NIR irradiation was analyzed by annexin-V and 7AAD staining (left panel). Mean percentages of early-apoptotic cells (annexin-V$^+$7AAD$^-$ cells) and late-apoptotic/necrotic cells (annexin-V$^+$7AAD$^+$ cells) are shown (right panel). # $p < 0.05$, ## $p < 0.01$ for early-apoptotic cells; * $p < 0.05$, ** $p < 0.01$ for late-apoptotic/necrotic cells. (b) Apoptosis of HeLa cells following treatment with fucoidan, CuS, and F-CuS with or without NIR irradiation was analyzed through flow cytometry. The mean percentages of early-apoptotic cells (annexin-V$^+$7AAD$^-$ cells) and late-apoptotic/necrotic cells (annexin-V$^+$7AAD$^+$ cells) are shown (right panel). # $p < 0.05$, ## $p < 0.01$ for early-apoptotic cells; * $p < 0.05$, ** $p < 0.01$ for late-apoptotic/necrotic cells.

28

Consistent with the F-CuS effect in HeLa cells, A549 cells also showed dramatic increases in early and late apoptosis following treatment with F-CuS and NIR irradiation (Figure 11). However, we found that fucoidan alone induced apoptosis in neither HeLa nor A549 cells at a given concentration (i.e., 75 ng/mL). We assume that these findings were due to the low concentration of fucoidan alone. According to previous reports, 10–200 μg/mL fucoidan effectively induces cell apoptosis [13, 15, 37, 38], but we used a mere 75 ng/mL of fucoidan by LbL coating with NPs. It should be noted that F-CuS without NIR irradiation induced a slightly higher rate of apoptosis in HeLa and A549 cells, compared to that of fucoidan alone at the same dose. This elevated apoptotic effect of F-CuS may be due to the improved cellular uptake of fucoidan, since F-CuS formulation led to higher amounts of intracellular fucoidan delivery compared to that of fucoidan alone, even at a relatively low concentration [39].
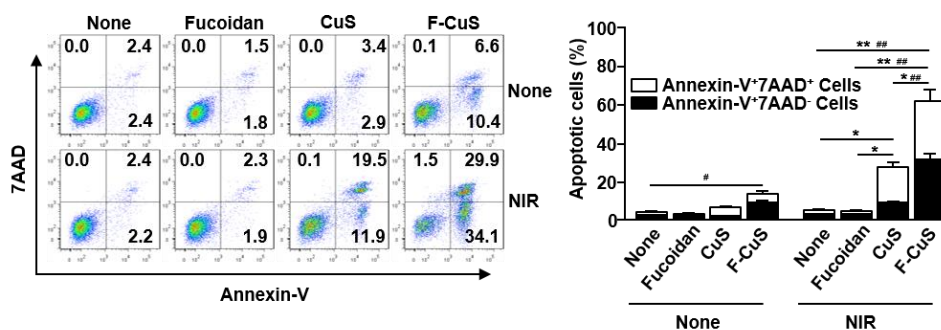
Figure 11. Apoptotic effect of F-CuS with laser irradiation against A549 cells. A549 cells (2×10^5) were incubated with fucoidan, CuS and F-CuS-FITC and irradiated with 808 nm laser for 5 min. Apoptosis of A549 cells were analyzed by annexin-V and 7AAD staining on a flow cytometry after 24 h of laser irradiation (left panel). Mean percentage of early apoptotic cells (Annexin-V$^+$7AAD$^-$ Cells) and late apoptotic/necrotic cells (Annexin-V$^+$7AAD$^+$ Cells) were shown (right panel). # $p < 0.05$, ## $p < 0.01$ early apoptotic cells, * $p < 0.05$, ** $p < 0.01$ late apoptotic/necrotic cells. Data are representative of or the average of analyses of 6 independent samples (2 samples per experiment, 3 independent experiments).

To further determine the apoptotic effect of F-CuS, we studied the apoptosis signaling pathway, including mitochondrial permeability and caspase-3 activation.
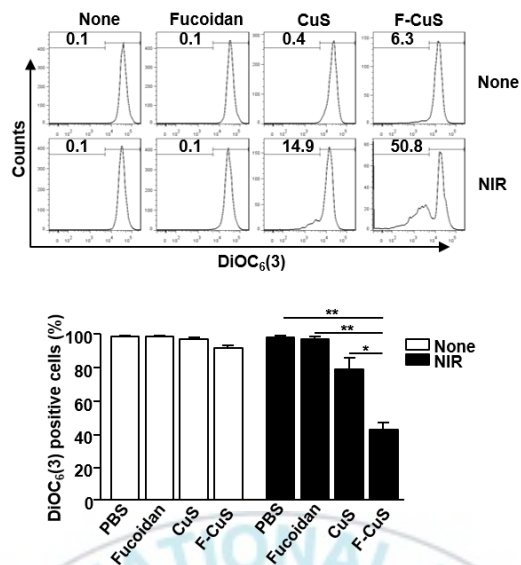
Figure 12. Mitochondria permeability of HeLa cells by F-CuS. HeLa cells (2×10^5) were incubated with fucoidan, CuS and F-CuS-FITC and irradiated with 808 nm laser for 5 min. Mitochondria permeability was measured by $DiOC_6(3)$ reduction in flow cytometry; $* p < 0.05$, $** p < 0.01$.

   NIR irradiation in F-CuS-treated cells induced marked increases in both mitochondrial permeability (Figure 12) and caspase-3 activity (Figure 13), compared to those of non-irradiated or fucoidan alone controls. Such increased effects of apoptotic activities were significantly stronger than those in the CuS-induced samples (Figures 12 and 13).

31
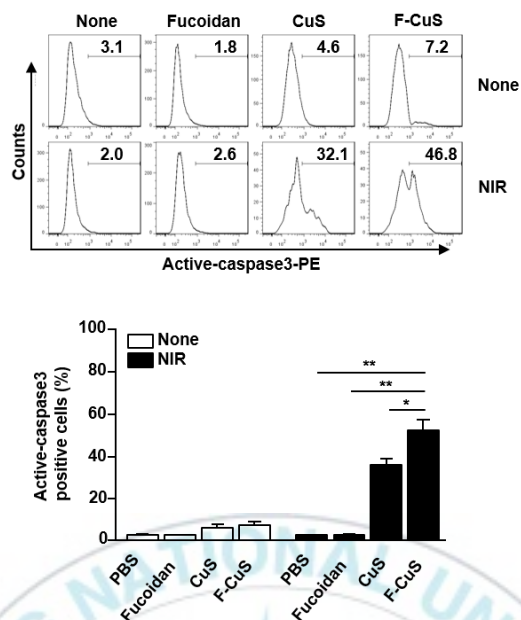
Figure 13. Activation of caspase-3 by F-CuS. HeLa cells (2×10^5) were incubated with fucoidan, CuS and F-CuS-FITC and irradiated with 808 nm laser for 5 min. Activation of caspase-3 was analyzed by flow cytometry, and the mean percentages of positive cells are shown; * $p < 0.05$, ** $p < 0.01$. All data are representative of, or the average of, analyses of six independent samples (i.e., two samples per experiment, three independent experiments).

The F-CuS was engineered to have pH-responsive drug delivery nanostructures, as fucoidan will be gradually released from the system when NPs are taken up by cancer cells in an acidic environment [35]. At such a lower pH, fucoidan sulfates become protonated, and electrostatic

interaction between PAH and fucoidan will consequently weaken [18]. In this pH-responsive manner, fucoidan will be free-form to induce apoptosis in the intracellular areas of cells. This explains why CuS did not efficiently promote apoptosis in HeLa and A549 cells, compared to F-CuS. In addition, the effect of fucoidan in promoting mitochondria-dependent apoptosis in cancer cells has been already been well determined [11, 13-15]. Thus, these data suggest that F-CuS promotes the enhanced intracellular delivery of fucoidan and NIR irradiation in F-CuS-treated cells, inducing apoptosis in cancer cells through the fucoidan-induced apoptotic effect and the hyperthermic effect.

3.5. F-CuS-mediated chemo–photothermal therapy *in vivo*

Our data, where F-CuS treatment with NIR irradiation induced apoptosis in HeLa and A549 cells, encouraged us to examine the therapeutic effect of F-CuS against tumors in a mouse model. Nude mice were subcutaneously (*s.c.*) xenografted with HeLa or A549 cells. Once tumors were well established 14 d after cell implantation, mice received an intratumoral (*i.t.*) injection of PBS, 4 μg/kg fucoidan, 10 mg/kg CuS, or 2.5 mg/kg F-CuS. Two hours after administration, PBS, CuS, and F-CuS-treated mice were irradiated for 5 min with an 808 nm laser (2 W/cm^2), and were monitored for tumor growth.
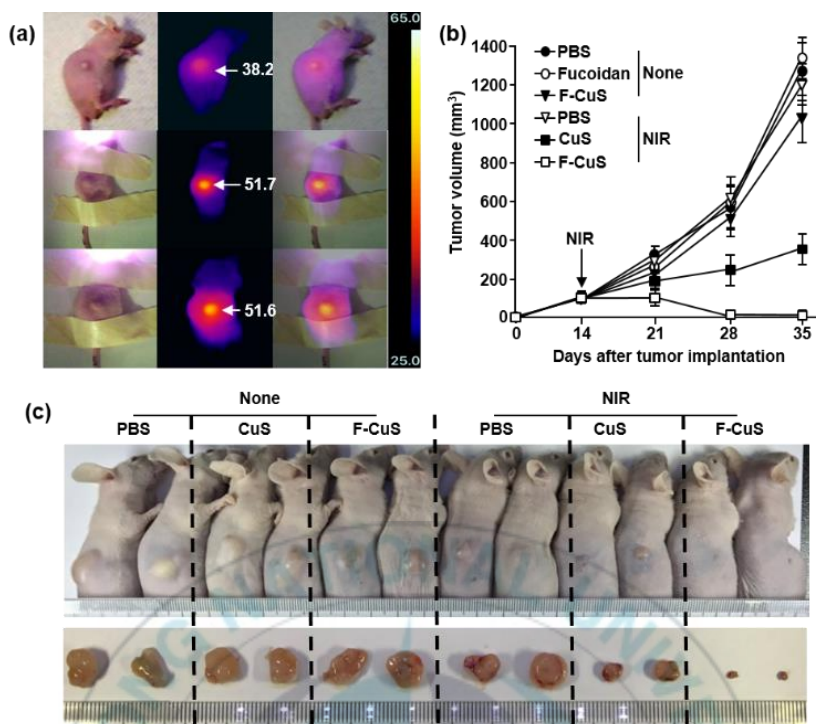
Figure 14. *In vivo* chemo–photothermal therapy of F-CuS against HeLa. Nude mice were injected *s.c.* with 5 x 10^6 HeLa cells. Once tumors were measured ~5.0 mm after 14 days, the mice were treated *i.t.* with 40 μg/kg fucoidan, 10 mg/kg CuS and 2.5 mg/kg F-CuS. Two hours after treatment, the mice were irradiated by 808 nm laser at 2 W/cm² for 5 min. (a) Thermal images of HeLa tumor mice are shown after NIR irradiation. (b) Tumor volumes of mice injected with HeLa were measured. (c) Tumor masses in the mice are shown after the mice were sacrificed on day 35 of HeLa cell xenograft. All data are representative of, or the average of, analyses of six independent samples (*i.e.*, two samples per experiment, three independent experiments).

As shown in the photothermal images in Figures 14a and 14a, there was a substantial NIR irradiation-induced temperature increase in the CuS and F-CuS-treated HeLa and A549 tumors from 25 ℃ to 51 ℃ or higher, while PBS-injected tumors showed slight skin-temperature increases of up to 38 ℃ under NIR irradiation. After NIR irradiation, the size of each HeLa and A549 tumor was gradually reduced in the F-CuS-treated mice (Figures 14b and 15b). On day 35 of tumor injection, the HeLa and A549 tumors had almost disappeared with F-CuS treatment combined with NIR irradiation (Figures 14c and 15c). Although CuS-treated mice with HeLa or A549 tumors also showed remarkably inhibited tumor growth compared to PBS or fucoidan alone-treated controls, the F-CuS treatment promoted a more efficient therapeutic effect than did the CuS treatment (Figures 14c and 15c).
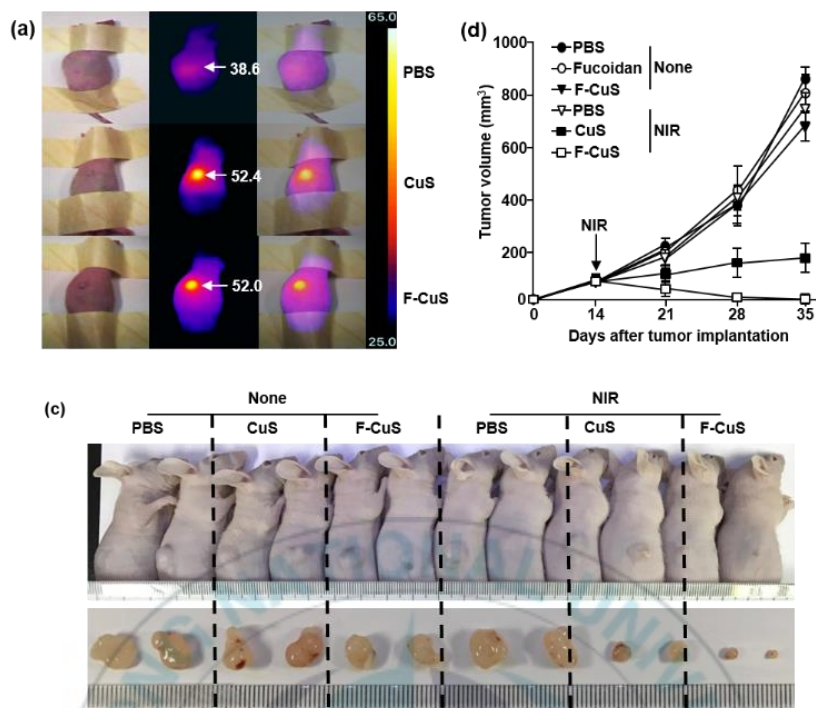
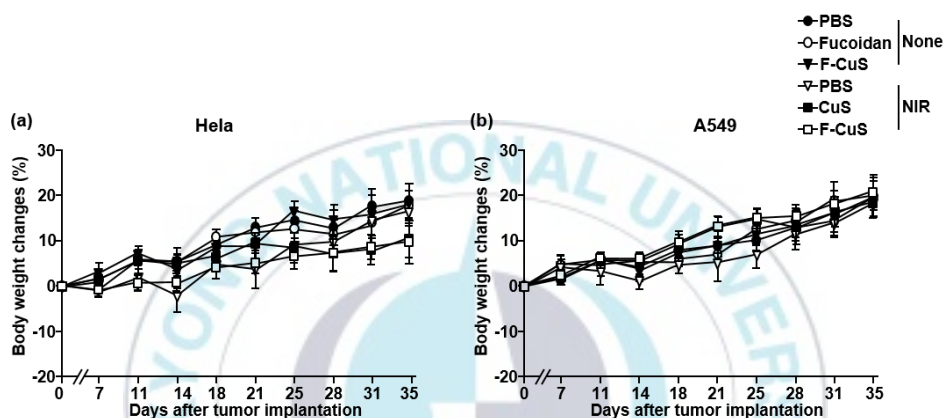**Figure 15.** *In vivo* chemo–photothermal therapy of F-CuS against A549. Nude mice were injected *s.c.* with 5 x 10^6 A549 cells. Once tumors were measured ~5.0 mm after 14 days, the mice were treated *i.t.* with 40 μg/kg fucoidan, 10 mg/kg CuS and 2.5 mg/kg F-CuS. Two hours after treatment, the mice were irradiated by 808 nm laser at 2 W/cm^2 for 5 min. (a) Thermal images of A549 tumor mice are shown after NIR irradiation. (b) Tumor volumes of mice injected with A549 were measured. (c) Tumor masses in the mice are shown after the mice were sacrificed on day 35 of A549 cell xenograft. All data are representative of, or the average of, analyses of six independent samples (*i.e.*, two samples per experiment, three independent experiments).

36

During the HeLa and A549 tumor therapy featuring the use of F-CuS and NIR irradiation, we also measured changes in body weight to evaluate the cytotoxic effect in mice; we found that neither CuS nor F-CuS with NIR irradiation alters body weight, compared to PBS or fucoidan-treated mice (Figure 16).

Figure 16. Changes of body weight during treatment of HeLa and A549 tumor by F-CuS. Nude mice were injected *s.c.* with 5 x 10^6 HeLa cells and 5 x 10^6 A549 cells, respectively. Once tumors were measured ~5.0 mm after 14 days, the mice were treated *i.t.* with 40 µg/kg fucoidan, 10 mg/kg CuS and 2.5 mg/kg F-CuS. Two hours after treatment, the mice were irradiated by 808 nm laser at 2 W/cm^2 for 5 min. The body weight of (a) HeLa and (b) A549 tumor implanted mice were measured during treatment of the tumor. Data are an average of analyses of 6 independent samples (2 mice per experiment, total 3 independent experiments).

In addition, the F-CuS treatment did not promote immune cell infiltration in the peripheral tissues, thus indicating that F-CuS treatment did not induce tissue inflammation (Figure 17). Thus, these *in vivo* results support the assertion that the use of F-CuS in combination with NIR irradiation efficiently promotes therapeutic effects against HeLa and A549 tumors in mice, without any adverse side effects (*e.g.*, body weight loss or inflammation of peripheral tissues).
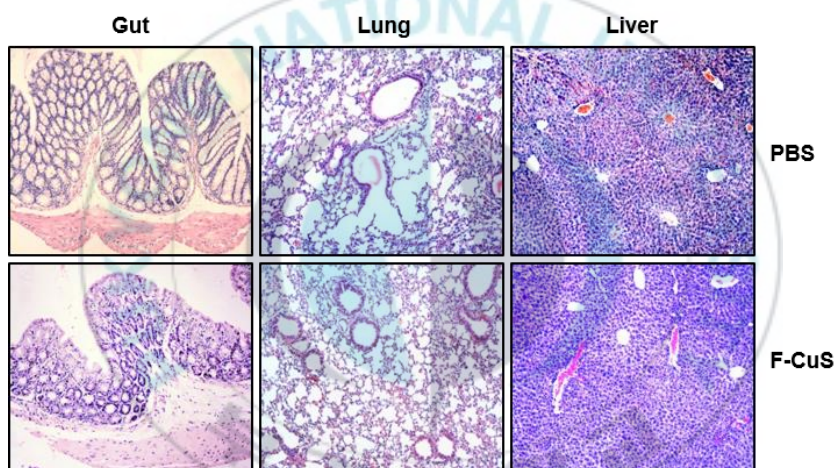
Figure 17. Histological analysis of peripheral tissue damage. HeLa tumor-bearing nude mice were treated *i.t.* with F-CuS and irradiated by 808nm laser at 2 W/cm^2 for 5 min. Twenty-one days after F-CuS treatment and laser irradiation, Gut, lung and liver were harvested and stained with haematoxylin and eosin (H&E). Data are representative of analyses of 6 independent samples (2 mice per experiment, total 3 independent experiments).

3.6. Therapeutic effect of F-CuS against multi-drug-resistant K562 cells

Since K562 cells are well known as multi-drug-resistant suspension cells, we next examined the effect of F-CuS in inducing cell death, *via* NIR irradiation and the intracellular delivery of fucoidan. K562 cells were treated with FITC-conjugated fucoidan or F-CuS, and 2 h later we measured cellular FITC signals. F-CuS-treated cells exhibited much higher intracellular fluorescence FITC intensity than the controls, including fucoidan alone-treated cells (Figure 18). These data give us confidence that F-CuS could be a suitable multi-therapeutic material against K562 cells.
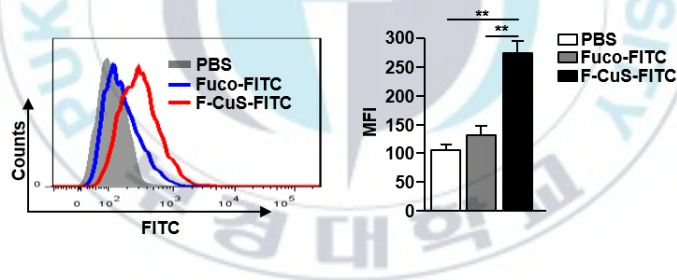
Figure 18. Intracellular uptake of fucoidan in K562 cells by F-CuS. K562 cells (2×10^5) were incubated with fucoidan-FITC (Fuco-FITC) and F-CuS-FITC for 2 h. The intracellular uptake of fucoidan was analyzed on a flow cytometry (left panel). Mean fluorescence intensity (MFI) of FITC positivecells was shown (right panel), ** $p < 0.01$. Data are representative of or theaverage of analyses of 6 independent samples (2 samples per experiment, 3 independent experiments).

Next, we evaluated the apoptotic effect of F-CuS with or without NIR irradiation. Consistent with the findings for other cell lines (HeLa and A549), 50 or 100 μg/mL of F-CuS induced considerable increases in apoptosis in K562 cells (Figure 19a). Moreover, cells treated with 50 μg/mL of F-CuS showed substantial increases in early apoptosis and late apoptosis/necrosis under 5 min of 808 nm laser irradiation (2.5 W/cm^2) (Figure 19a). However, 100 μg/mL F-CuS with NIR irradiation induced late apoptosis/necrosis without early apoptosis. In addition, NIR irradiation in 50 μg/mL F-CuS-treated K562 cells promoted significantly higher early-apoptosis and late-apoptosis/necrosis cell populations, compared to CuS-treated K562 cells (Figure 19b). Thus, these data suggest that F-CuS administration in conjunction with NIR irradiation also triggers the promotion of apoptosis in multidrug-resistant cells (*i.e.*, K562).
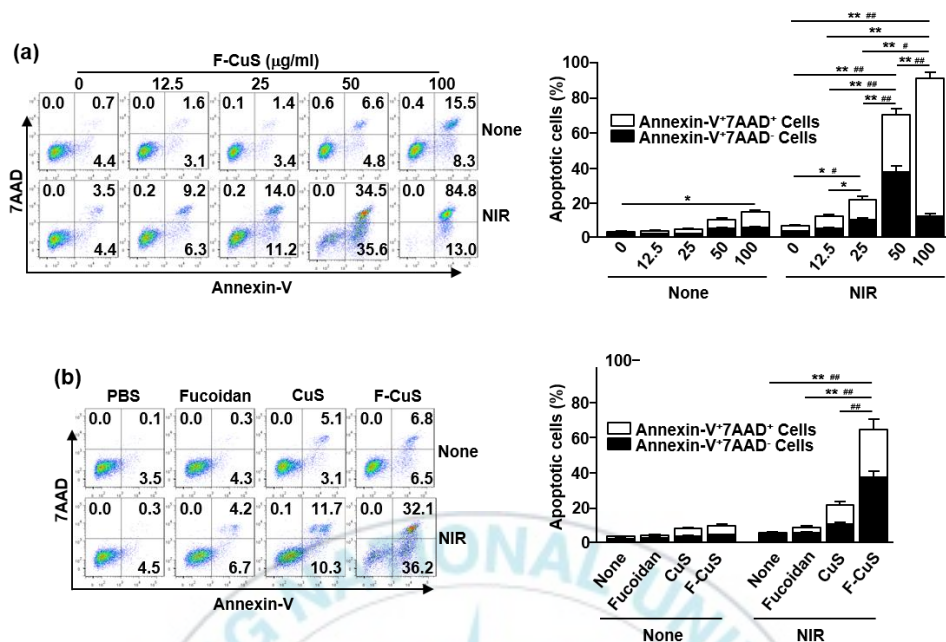
Figure 19. Apoptotic effect of F-CuS with laser irradiation against multi-drug-resistant K562 cells. (a) K562 cells (2×10^5) were treated with an indicated dose of F-CuS for 2 h; cells were irradiated for 5 min with an 808 nm laser at 2.5 W/cm^2. Apoptosis of K562 cells was analyzed by annexin-V & 7AAD staining (left panel). (b) K562 cells were treated with 75 ng/mL fucoidan, 200 μg/mL CuS, or 50 μg/mL F-CuS for 2 h, and then the cells were irradiated for 5 min with an 808 nm laser at 2.5 W/cm^2. Apoptotic K562 cells are shown (left panel). In (a) and (b), the mean percentages of early-apoptotic cells (annexin-V$^+$7AAD$^-$ cells) and late-apoptotic/necrotic cells (annexin-V$^+$7AAD$^+$ cells) are shown (right panel). # $p < 0.05$, ## $p < 0.01$ for early-apoptotic cells; * $p < 0.05$, ** $p < 0.01$ for late-apoptotic/necrotic cells (right panel).

41

We then examined the elimination of K562 cells in the mouse model. Nude mice were *s.c.* xenografted with K562 cells. Two weeks after tumor implantation, mice were treated with an *i.t.* injection of PBS, 40 μg/kg fucoidan, 10 mg/kg CuS, or 2.5 mg/kg F-CuS for 2 h, and irradiated for 5 min with an 808 nm laser (2.5 W/cm^2). As shown in Figure 20a, NIR irradiation promoted remarkable increases in temperature in the CuS and F-CuS-treated tumors, whereas negligible temperature increases were observed in the PBS-treated mice. Moreover, tumors completely disappeared in F-CuS-treated mice on day 28 of tumor injection, whereas tumors were still apparent in the CuS-treated mice—although they were smaller, to some extent, than those of other controls (Figures 20b and c).
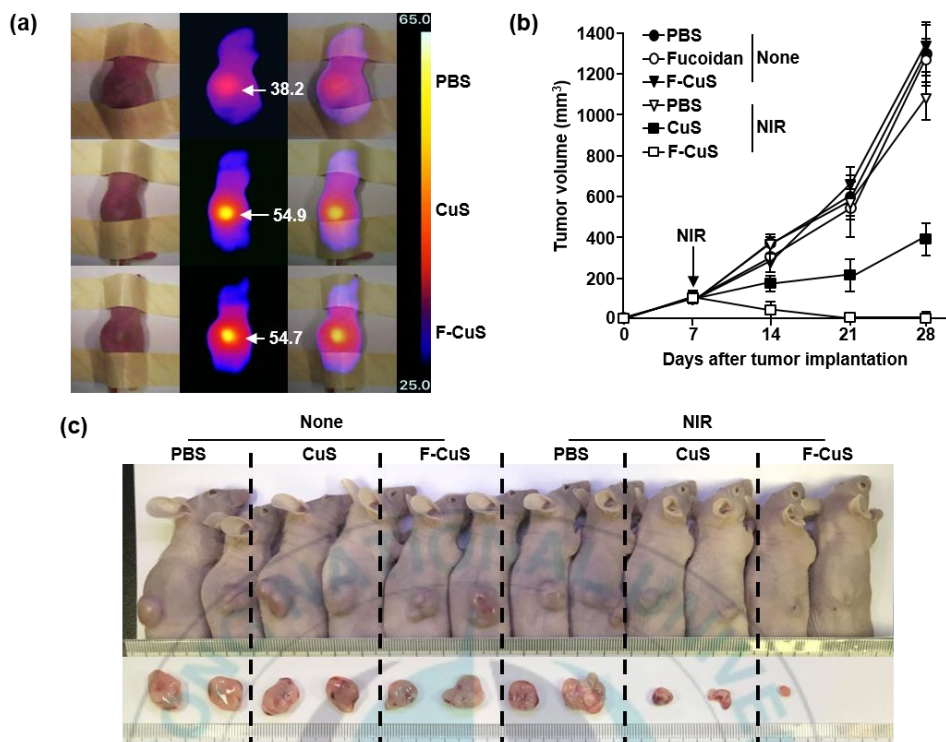
Figure 20. *In vivo* chemo–photothermal therapy of F-CuS against multi-drug-resistant K562. Nude mice were injected *s.c.* with 5×10^6 K562 cells. Once tumors measured to be ~5.0 mm (after 14 d), the mice were treated *i.t.* with 4 µg/kg fucoidan, 10 mg/kg CuS, or 2.5 mg/kg F-CuS. Two hours after treatment, the mice were irradiated for 5 min with an 808 nm laser at 2.5 W/cm^2. (a) Thermal images of mice are shown after NIR irradiation. (b) Tumor volumes are shown. (c) Tumor masses in the mice are shown on day 28 of NIR irradiation. Data are representative of analyses of four independent samples (*i.e.*, two mice per experiment, two independent experiments).

Furthermore, treatment with F-CuS and NIR irradiation did not induce body

weight loss in the mice during treatment (Figure 21).
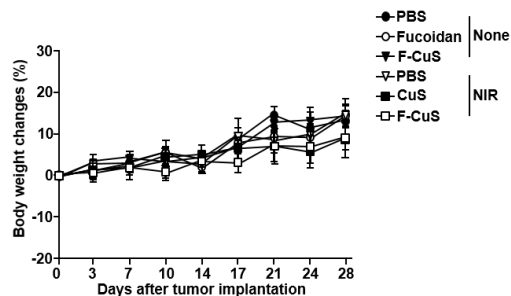
Figure 21. Changes of body weight during treatment of K562 tumor by F-CuS. Nude mice were injected *s.c.* with 5 x 10^6 K562 cells. Fourteen days after tumor injection, the mice were treated *i.t.* with 40 μg/kg fucoidan, 10 mg/kg CuS and 2.5 mg/kg F-CuS. Two hours after treatment, the mice were irradiated by 808 nm laser at 2.5 W/cm^2 for 5 min. The body weight of the mice were monitored during treatment of the tumor. Data are an average of analyses of 6 independent samples (2 mice per experiment, total 3 independent experiments).

Previous research has shown that fucoidan does not promote apoptosis

in K562 cells. Moreover, the apoptosis-signaling pathway in K562 cells—

including the ERK, JNK, and caspase-signaling pathway—was found not

to be activated by fucoidan [11]. In the current study, we found that F-CuS

promoted considerable apoptosis in K562 cells, even in the absence of NIR

irradiation. Compared to HeLa and A549 cells (Figure 8), K562 cells did not take up fucoidan intracellularly (Figure 18); this suggests that drug resistance against fucoidan-induced apoptosis may be due to the failure to take up fucoidan intracellularly. In the current study, F-CuS efficiently delivered fucoidan into the intracellular areas of K562 cells, resulting in induced cell apoptosis; this may be due to the intracellular delivery of fucoidan by NPs. Therefore, we concluded that the chemo and phototherapeutic effect of F-CuS was also applicable to multi-drug-resistant K562 cells. In future research, we will investigate the apoptotic effect of F-CuS without NIR irradiation, and whether a high concentration of F-CuS can induce apoptosis in K562 cells and activate apoptotic signaling.

4. Conclusion

To derive an enhanced therapy by which to cure cancer, we prepared nanoparticles *via* a layer-by-layer technique, where near-infrared (NIR)-absorbing inorganic material was coated with a natural anti-cancer agent. We demonstrated that our material can induce apoptosis in cancer cells by combining the fucoidan-mediated anti-cancer effect and the NIR-induced hyperthermic effect; this combination consequently eliminated multiple tumors in live mouse models. Thus, this chemo–photothermal therapy, which uses NIR-absorbing NPs and a biologically active component, will be a promising candidate in the fields of material sciences and cancer nanotechnology.

References

[1] M. Chidambaram, R. Manavalan, K. Kathiresan, Nanotherapeutics to overcome conventional cancer chemotherapy limitations, Journal of Pharmacy & Pharmaceutical Sciences 14(1) (2011) 67-77.

[2] L. Cunha, A. Grenha, Sulfated Seaweed Polysaccharides as Multifunctional Materials in Drug Delivery Applications, Marine drugs 14(3) (2016).

[3] T. Nishino, C. Nishioka, H. Ura, T. Nagumo, Isolation and partial characterization of a novel amino sugar-containing fucan sulfate from commercial Fucus vesiculosus fucoidan, Carbohydrate Research 255 (1994) 213-224.

[4] A.D. Holtkamp, S. Kelly, R. Ulber, S. Lang, Fucoidans and fucoidanases—focus on techniques for molecular structure elucidation and modification of marine polysaccharides, Applied Microbiology and Biotechnology 82(1) (2009) 1.

[5] W. Black, E. Dewar, F. Woodward, Manufacture of algal chemicals. IV—laboratory-scale isolation of fucoidin from brown marine algae, Journal of the Science of Food and Agriculture 3(3) (1952) 122-129.

[6] M.S. Patankar, S. Oehninger, T. Barnett, R.L. Williams, G.F. Clark, A revised structure for fucoidan may explain some of its biological activities, Journal of Biological Chemistry 268(29) (1993) 21770-21776.

[7] B. Li, F. Lu, X. Wei, R. Zhao, Fucoidan: structure and bioactivity, Molecules 13(8) (2008) 1671-95.

[8] J. Durig, T. Bruhn, K.H. Zurborn, K. Gutensohn, H.D. Bruhn, L. Beress, Anticoagulant fucoidan fractions from Fucus vesiculosus induce platelet activation in vitro, Thrombosis research 85(6) (1997) 479-91.

[9] K. Hayashi, J.B. Lee, T. Nakano, T. Hayashi, Anti-influenza A virus characteristics of a fucoidan from sporophyll of Undaria pinnatifida in mice with normal and compromised immunity, Microbes and infection 15(4) (2013) 302-9.

[10] J.O. Jin, H.Y. Park, Q. Xu, J.I. Park, T. Zvyagintseva, V.A. Stonik, J.Y. Kwak, Ligand of scavenger receptor class A indirectly induces maturation of human blood dendritic cells via production of tumor necrosis factor-alpha, Blood 113(23) (2009) 5839-47.

[11] J.O. Jin, M.G. Song, Y.N. Kim, J.I. Park, J.Y. Kwak, The mechanism of fucoidan-induced apoptosis in leukemic cells: involvement of ERK1/2, JNK, glutathione, and nitric oxide, Molecular carcinogenesis 49(8) (2010) 771-82.

[12] J.O. Jin, W. Zhang, J.Y. Du, K.W. Wong, T. Oda, Q. Yu, Fucoidan can function as an adjuvant in vivo to enhance dendritic cell maturation and function and promote antigen-specific T cell immune responses, PLoS One 9(6) (2014) e99396.

[13] H.J. Boo, J.H. Hyun, S.C. Kim, J.I. Kang, M.K. Kim, S.Y. Kim, H. Cho, E.S. Yoo, H.K. Kang, Fucoidan from Undaria pinnatifida induces apoptosis in A549 human lung carcinoma cells, Phytotherapy Research 25(7) (2011) 1082-6.

[14] S. Chen, Y. Zhao, Y. Zhang, D. Zhang, Fucoidan induces cancer cell apoptosis by modulating the endoplasmic reticulum stress cascades, PLoS One 9(9) (2014) e108157.

[15] Z. Zhang, K. Teruya, H. Eto, S. Shirahata, Fucoidan extract induces apoptosis in MCF-7 cells via a mechanism involving the ROS-dependent JNK activation and mitochondria-mediated pathways, PLoS One 6(11) (2011) e27441.

[16] L. Bachelet-Violette, A.K. Silva, M. Maire, A. Michel, O. Brinza, P. Ou, V. Ollivier, A. Nicoletti, C. Wilhelm, D. Letourneur, Strong and specific interaction of ultra small superparamagnetic iron oxide nanoparticles and human activated platelets mediated by fucoidan coating, RSC Advances 4(10) (2014) 4864-4871.

[17] Y.C. Huang, R.Y. Li, Preparation and characterization of antioxidant nanoparticles composed of chitosan and fucoidan for antibiotics delivery, Marine drugs 12(8) (2014) 4379-98.

[18] K.-Y. Lu, R. Li, C.-H. Hsu, C.-W. Lin, S.-C. Chou, M.-L. Tsai, F.-L. Mi, Development of a new type of multifunctional fucoidan-based nanoparticles for anticancer drug delivery, Carbohydrate Polymers 165 (2017) 410-420.

[19] Q. Ban, T. Bai, X. Duan, J. Kong, Noninvasive photothermal cancer therapy nanoplatforms via integrating nanomaterials and functional polymers, Biomaterials science (2016).

[20] Z. Bao, X. Liu, Y. Liu, H. Liu, K. Zhao, Near-infrared light-responsive inorganic nanomaterials for photothermal therapy, Asian Journal of Pharmaceutical Sciences 11(3) (2016) 349-364.

[21] N. Biosciences, Inc. Efficacy study of AuroLase therapy in subjects with primary and/or metastatic lung tumors, ClinicalTrials. gov [Internet]; National Library of Medicine: Bethesda, MD (2000).

[22] B. Staves, Pilot study of Aurolase™ therapy in refractory and/or recurrent tumors of the head and neck, 2010.

[23] C. Tortiglione, R. Iachetta, Playing with nanoparticle shapes and laser powers to decide which route to take during photothermal therapy: apoptosis or necrosis?, Annals of Translational Medicine 4(Suppl 1) (2016).

[24] S. Goel, F. Chen, W. Cai, Synthesis and biomedical applications of copper sulfide nanoparticles: from sensors to theranostics, Small 10(4) (2014) 631-45.

[25] V. Groh, Y.Q. Li, D. Cioca, N.N. Hunder, W. Wang, S.R. Riddell, C. Yee, T. Spies, Efficient cross-priming of tumor antigen-specific T cells by dendritic cells sensitized with diverse anti-MICA opsonized tumor cells, Proceedings of the National Academy of Sciences of the United States of America 102(18) (2005) 6461-6.

[26] J.T. Opferman, S.J. Korsmeyer, Apoptosis in the development and maintenance of the immune system, Nature immunology 4(5) (2003) 410-5.

[27] J.R. Melamed, R.S. Edelstein, E.S. Day, Elucidating the fundamental mechanisms of cell death triggered by photothermal therapy, ACS Nano 9(1) (2015) 6-11.

[28] X. Li, C. Liu, S. Wang, J. Jiao, D. Di, T. Jiang, Q. Zhao, S. Wang, Poly(acrylic acid) conjugated hollow mesoporous carbon as a dual-stimuli triggered drug delivery system for chemo-photothermal synergistic therapy, Materials science & engineering. C, Materials for biological applications 71 (2017) 594-603.

[29] A. Yuan, W. Huan, X. Liu, Z. Zhang, Y. Zhang, J. Wu, Y. Hu, NIR Light-Activated Drug Release for Synergetic Chemo-Photothermal Therapy, Molecular pharmaceutics (2016).

[30] L. Zhang, H. Su, J. Cai, D. Cheng, Y. Ma, J. Zhang, C. Zhou, S. Liu, H. Shi, Y. Zhang, C. Zhang, A Multifunctional Platform for Tumor Angiogenesis-Targeted Chemo-Thermal Therapy Using Polydopamine-Coated Gold Nanorods, ACS Nano 10(11) (2016) 10404-10417.

[31] V.M. Rumjanek, G.S. Trindade, K. Wagner-Souza, M.C. de-Oliveira, L.F. Marques-Santos, R.C. Maia, M.A. Capella, Multidrug resistance in tumour cells: characterization of the multidrug resistant cell line K562-Lucena 1, Anais da Academia Brasileira de Ciencias 73(1) (2001) 57-69.

[32] M. Zhou, R. Zhang, M. Huang, W. Lu, S. Song, M.P. Melancon, M. Tian, D. Liang, C. Li, A chelator-free multifunctional [64Cu]CuS nanoparticle platform for simultaneous micro-PET/CT imaging and photothermal ablation therapy, Journal of the American Chemical Society 132(43) (2010) 15351-8.

[33] G.A. Dominguez, S.E. Lohse, M.D. Torelli, C.J. Murphy, R.J. Hamers, G. Orr, R.D. Klaper, Effects of charge and surface ligand properties of nanoparticles on oxidative stress and gene expression within the gut of Daphnia magna, Aquatic toxicology 162 (2015) 1-9.

[34] G. Schneider, G. Decher, From Functional Core/Shell Nanoparticles Prepared via Layer-by-Layer Deposition to Empty Nanospheres, Nano letters 4(10) (2004) 1833-1839.

[35] S. Manchun, C.R. Dass, P. Sriamornsak, Targeted therapy for cancer using pH-responsive nanocarrier systems, Life sciences 90(11-12) (2012) 381-7.

[36] J.F. Kerr, A.H. Wyllie, A.R. Currie, Apoptosis: a basic biological phenomenon with wide-ranging implications in tissue kinetics, British journal of cancer 26(4) (1972) 239-57.

[37] F.R. Stevan, M.B. Oliveira, D.F. Bucchi, Noseda, M. Iacomini, M.E. Duarte, Cytotoxic effects against HeLa cells of polysaccharides from seaweeds, Journal of submicroscopic cytology and pathology 33(4) (2001) 477-84.

[38] J. Ye, Y. Li, K. Teruya, Y. Katakura, A. Ichikawa, H. Eto, M. Hosoi, M. Hosoi, S. Nishimoto, S. Shirahata, Enzyme-digested Fucoidan Extracts Derived from Seaweed Mozuku of Cladosiphon novae-caledoniae kylin Inhibit Invasion and Angiogenesis of Tumor Cells, Cytotechnology 47(1-3) (2005) 117-26.

[39] K.S. Soppimath, T.M. Aminabhavi, A.R. Kulkarni, W.E. Rudzinski, Biodegradable polymeric nanoparticles as drug delivery devices, Journal of controlled release : official journal of the Controlled Release Society 70(1-2) (2001) 1-20.

Acknowledgements

I would like to express my deepest gratitude to my adviser Dr. Junghwan Oh, the professor of Department of Interdisciplinary program of Biomedical Mechanical & Electrical Engineering at Pukyong National University, for his invaluable guidance, support and encouragement toward the completion of the research and writing of this thesis. Dr. Oh have introduced me to the broad field of Biomedical Engineering research and I have learned the fundamental knowledge of the photoacoustics and photothermal therapy from him.

I deeply appreciate all the help and support from following professors, Dr. Jun-O Jin from Fudan University, Dr. Minseok Kwak from Department of Chemistry and Dr. Madhappan S. Moorthy. Especially Dr. Jun-O Jin, he has taught me well about the induction of apoptosis and photothermal therapy and supervised me a lot during the experiments and while writing this thesis. I would like to say thanks to him.

I would also like to thank all my schoolmates and friends from my lab, Dr. Yun-ok Oh, Mr. Han-su Suh, Dr. Bharathiraja, Quang, Tu, Nam, Phouc, Phong, Vy and Jeayeop. They have helped me a lot with my research and always have been such good friends. Also, I am grateful to my parents for their unending love, support and encouragement during two years of master.